

SUPPLEMENTARY INFORMATION FOR

Enzyme Redesign Guided by Cancer-Derived *IDH1* Mutations

Zachary J. Reitman, Bryan D. Choi, Ivan Spasojevic, Darell D. Bigner, John H. Sampson, Hai Yan

Supplementary Methods	2-3
Supplementary Results	
Supplementary Figure 1.	
Alignment of β -hydroxyacid oxidative decarboxylases.....	4-5
Supplementary Figure 2.	
Purification of <i>Sc</i> HIDH mutants.....	6
Supplementary Figure 3.	
Rate analysis of <i>Sc</i> HIDH mutants.....	7
Supplementary Figure 4.	
LC-MS/MS analysis of <i>Sc</i> HIDH reactivities.....	8
Supplementary Figure 5.	
<i>Sc</i> HIDH mutants stoichiometrically produce (<i>R</i>)-2-hydroxyadipate.....	9
Supplementary Figure 6.	
R118H mutation enhances <i>Tt</i> HIDH (<i>R</i>)-2-hydroxyadipate dehydrogenase activity	10
Supplementary References.....	11

SUPPLEMENTARY METHODS

Homology analysis. Structures were displayed in UCSF Chimera software version 1.5²⁴, using PDB 1T0L for *HsIDH1*¹⁸, 3TY3 for *SpHIDH*¹⁹, and 3ASJ for *TtHIDH*²⁵. Multiple Alignment using Fast Fourier Transform (MAFFT)²⁶ was used to align sequences using BLOSUM 30 matrix, 1.0 gap open penalty, and genafpair fourier transform settings. Alignments were drawn with ESPript²⁷, with secondary structure elements from *HsIDH1* (PBD 1T0L¹⁸) shown. GeneID was 49168486 for *HsIDH1*, 28178832 for *HsIDH2*, 2388955 for *SpHIDH*, 731845 for *ScHIDH*, 46199314 for *TtHIDH*, 1052977 for *SyIDH*, 209772816 for *EcIDH*, 729813 for *BsIDH*, 62897507 for *HsNAD-IDH*, 238879624 for *CaHIDH*, 320668365 for *EcTDH*, 167033202 for *PpTDH*, 66773874 for *TtIPMDH*, 198283840 for *TfIPMDH*, and 151943807 for *ScIPMDH*.

Chemicals. NADH reduced dipotassium salt (purity ≥95%), 2-oxoadipic acid (≥95%), 2-oxoglutarate sodium salt (≥98%), 2-heptandioic acid (≥98%), and (+)-diacetyl-L-tartaric anhydride (≥97%) were from Sigma. A racemic mixture of (*R*)- and (*S*)-2-hydroxyadipate was generated by reacting 1 mg 2-oxoadipic acid with 1mg NaBH₄ in 200 µl of anhydrous methanol at 60 °C for 30 min and characterization matched literature data⁶. [3,3,4,4]-²H₄-(*R/S*)-2-hydroxyglutarate (2HG-d4) was synthesized previously²¹.

Expression and purification of HIDH mutants. The gene encoding *ScHIDH* (LYS12, NC_001141.2) lacking a 3' STOP codon was amplified from an *S. cerevisiae* gDNA library. The gene encoding *TtHIDH* (TTC1012, NC_005835.1) lacking a 3' STOP codon was PCR amplified from a *T. thermophilus* HB27 gDNA library. These fragments were cloned into pTrcHis2-TOPO, which appends a C-terminal 6x His tag (Invitrogen). Mutagenesis was performed using the QuikChange Site Directed mutagenesis kit (Agilent). Procedures for expression and purification of homoisocitrate dehydrogenases were adapted from published methods¹⁰. Expression constructs were transformed into BL21-DE3 E. coli (Stratagene). A single colony was inoculated into 5 ml of LB-Amp media starter cultures and grown by shaking (225 rpm at 37 °C) for 6 h. 5 ml starter cultures were added to 45 ml of LB-Amp, shaken for 2 h, and shaken for an additional 2 h after induction with 1 mM IPTG. Pellets were harvested by centrifugation at 4500 x g at 4 °C and resuspended in 2 ml of buffer A (500 mM NaCl, 10 mM MgCl₂, 20 mM imidazole, 2 mM β-mercaptoethanol, 10 mM Tris, pH 7.5 supplemented with 1x EDTA-free Complete Mini protease inhibitor from Roche) on ice and sonicated for 6 cycles of 15 seconds each on ice on a Branson Sonifer 250 (Emerson). This crude lysate was cleared by centrifugation at 13,000 x g at 4 °C. Crude lysates were loaded on a Ni-NTA Spin Column (cat. No. 31014, Qiagen) that was preequilibrated with buffer A by spinning for 10 min at 300 x g at 4 °C. This was then washed with 10 column volumes of buffer A that was modified to contain 75 mM imidazole, 5% glycerol, and 0.1% Triton-X100 by spinning for 1 min at 900 x g. Eluates were obtained using buffer A that was modified to contain 500 mM imidazole. Eluates were brought to 10% glycerol and stored in aliquots at -80 °C for *ScHIDH* and at 4 °C for *TtHIDH*. Approximately 2.5 mg purified protein was obtained per g wet bacterial pellet. Purity was approximately 95% as assessed by SDS-PAGE stained with SilverQuest Silver Staining Kit (Life Technologies).

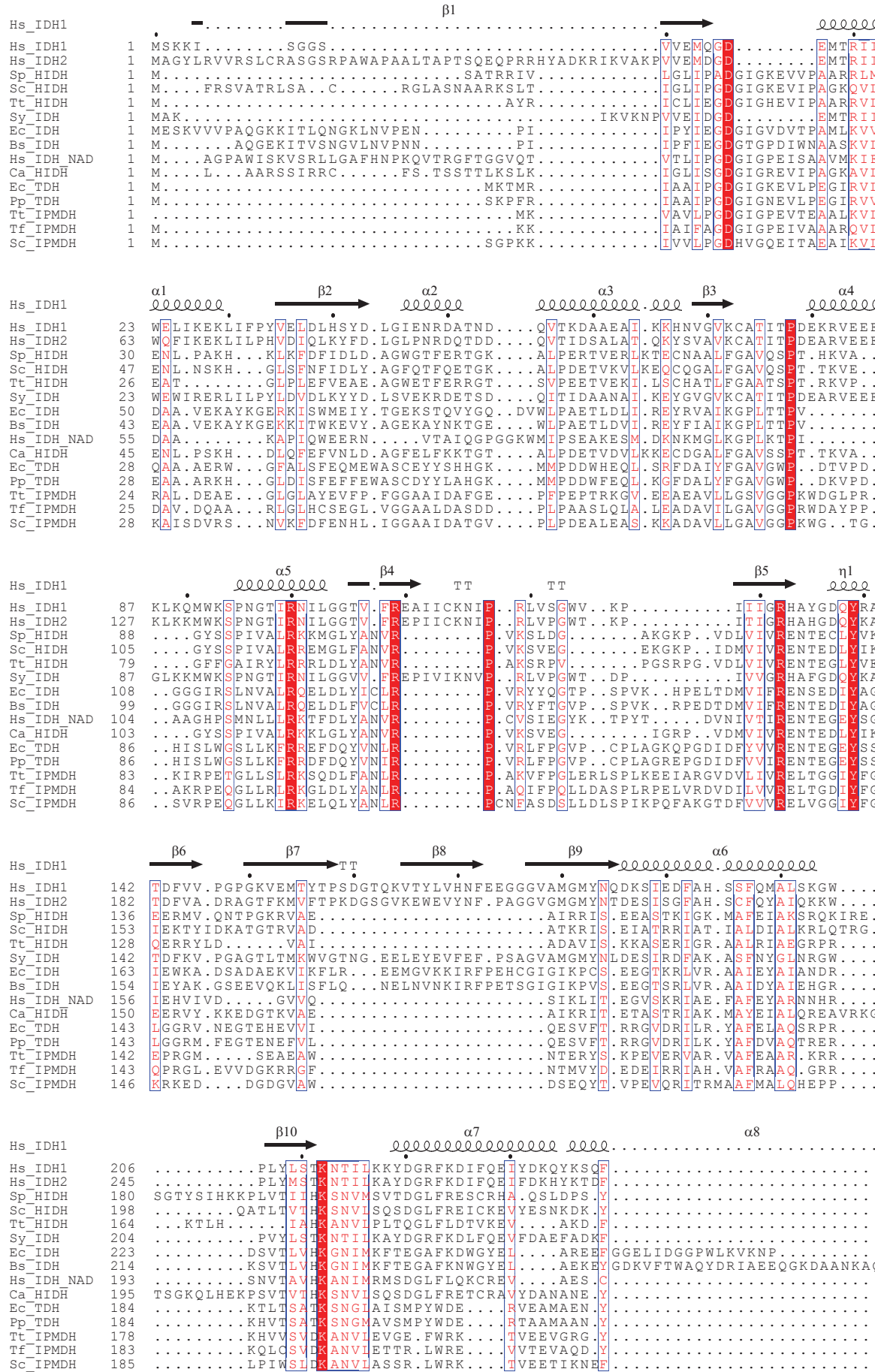
Activity measurement. Assays were performed with 40 ng/µl enzyme, 15 mM 2-oxoadipate, 100 µM NADH, 20 mM MgCl₂ and 100 mM HEPES, pH 7.3 in 10 or 20 µl in 384-well black microplates (788076, Greiner) unless otherwise specified. NADH was monitored by the decrease in fluorescence (ex. 340 nm, em. 450 nm) on a fluorescent plate reader. The levels of fluorescence were converted to NADH concentrations based on NADH standards. Reactions with high amounts of NADH (>300 µM) were monitored by the absorbance of NADH as indicated in the text, at 340 nm in a 40 µl reaction volume in a clear 96-well plate on the same plate reader. Reactions with *ScHIDH* were carried out at 25 °C and reactions with *TtHIDH* were carried out at 45 °C. Rates are initial rates from the first 10 minutes of reaction. For K_M determination, concentrations of substrate at least 5x higher than the K_M were used (for

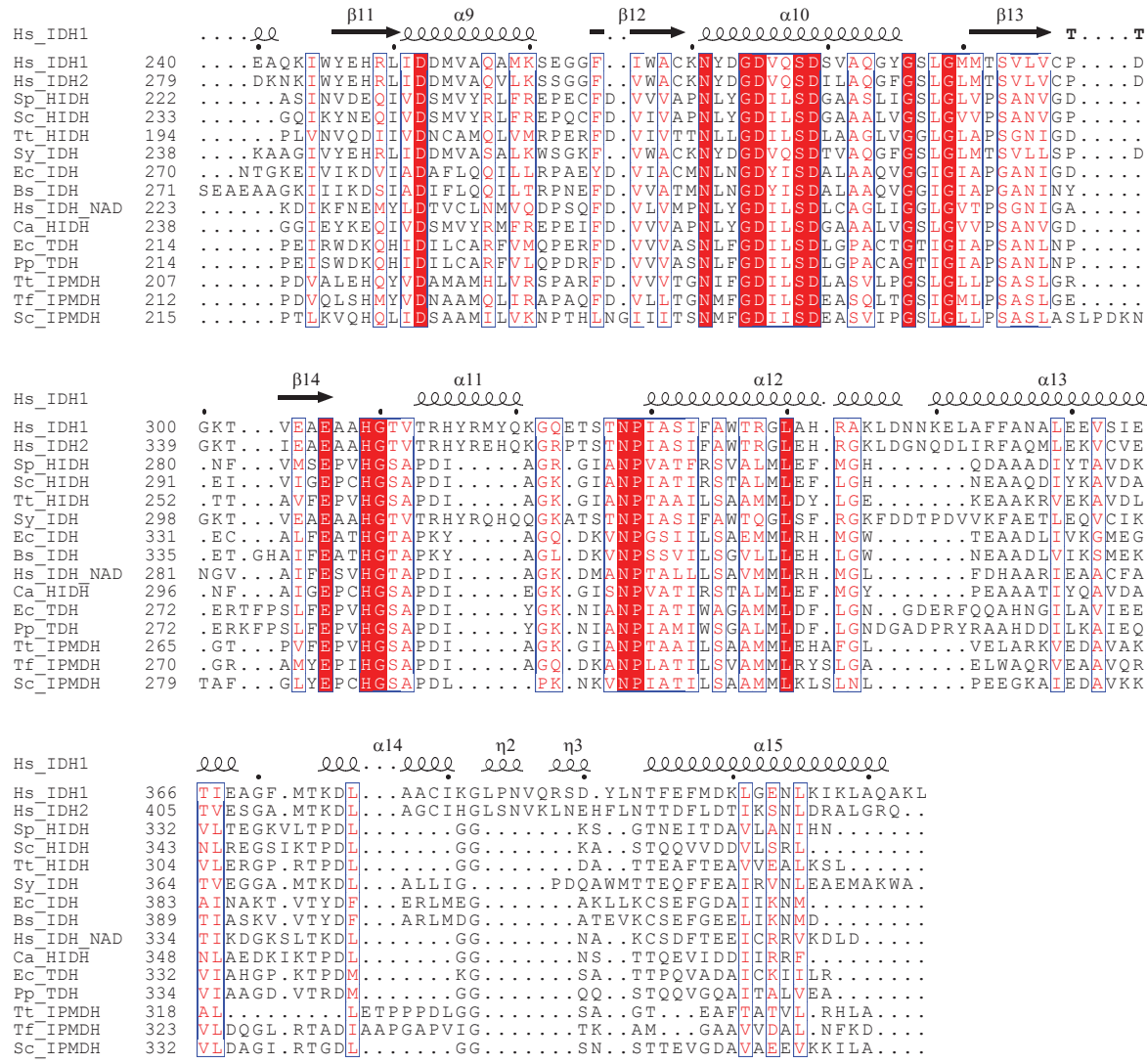
NADH, 500 μ M; for 2-oxoadipate, 15 mM) while the substrate of interest was varied in concentration. K_m and V_{max} were estimated by fitting data to equation (1), where X is substrate concentration and Y is rate, using nonlinear regression.

$$(1) \quad Y = V_{max} * X / (K_m + X)$$

LC-MS/MS. LC-MS/MS was based on the procedure described for 2-hydroxyglutarate^{20, 21}. To 20 μ L of reaction mix, 2 μ L of 130 μ g/mL of a racemic mixture of 2HG-d4 (internal standard) in water was added and the mixture dried by vacuum centrifuge (50 °C, 15 min). Dry residue was treated with 50 mg/mL freshly prepared diacetyl-L-tartaric anhydride in dichloromethane/glacial acetic acid (4/1 by volume) and heated (75 °C 30 min). After drying (50 °C, 15 min) the residue was dissolved in 100 μ L LC mobile phase A (see below) for analysis. An Agilent 1200 series HPLC (Santa Clara, CA) was used for liquid chromatography (LC) and a Sciex/Applied Biosystems API 3200 QTrap (Carlsbad, CA) was used for triple quadrupole mass spectrometry (MS/MS). Mobile phase A: water, 3% acetonitrile, 280 μ L ammonium hydroxide (~25%), pH adjusted to 3.6 by formic acid (~98%). Mobile phase B: methanol. Analytical column: Kinetex C₁₈, 150×4.6 mm, 2.6 μ m, and SafeGuard C₁₈ 4×3 mm guard-column from Phenomenex (Torrance, CA). Column temperature: 45 °C. Elution gradient at 1 mL/min flow rate: 0–1 min 0% B, 1–2 min 0–100% B, 2–3.5 min 100% B, 3.5–4 min 100–0% B, 4–10 min 0% B. Injection volume: 10 μ L. For initial product characterization, Q1/Q3 (*m/z*) transitions monitored were predicted based on the known fragmentation pattern of 2HG-d4^{20, 21} as shown in the mass fragmentation diagrams in **Supplementary Fig. 4**: 421.3/205.1, 421.3/187.0, 377.0/161.2, 377.0/143.2, 367.0/151.0, 367.0/132.0 for homoisocitrate transitions 1 and 2, 2-hydroxyadipate transitions 1 and 2, and 2HG-d4 transitions 1 and 2, respectively. For enantiospecific 2-hydroxyadipate quantification, Q1/Q3 (*m/z*) transitions monitored: 377/161 and 367/151 for 2-hydroxyadipate and 2HG-d4. To calibrate, 0, 1.6, 8, 40, 200, and 1000 μ g/ml 2-hydroxyadipate reacted with diacetyl-L-tartaric anhydride was analyzed in reaction buffer. (*R*) and (*S*) 2-hydroxyadipate enantiomers were discriminated based on time of elution from the HPLC column, using the relative elution time for (*R*)-2HG-d4 compared to the racemic mixture of 2HG-d4²¹. Standard samples were analyzed alongside experimental samples and accuracy acceptance criteria was 85% for each standard. The lower limit of quantification was taken as the concentration of the lowest standard.

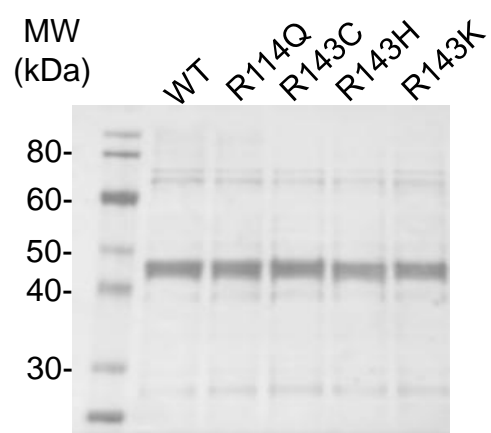
Statistical analysis. Activity measurements and LC-MS/MS analyses are representative of experiments were performed in triplicate unless otherwise specified. Data points in activity measurement plots represent mean \pm s.d. from n=2 reactions unless otherwise specified.





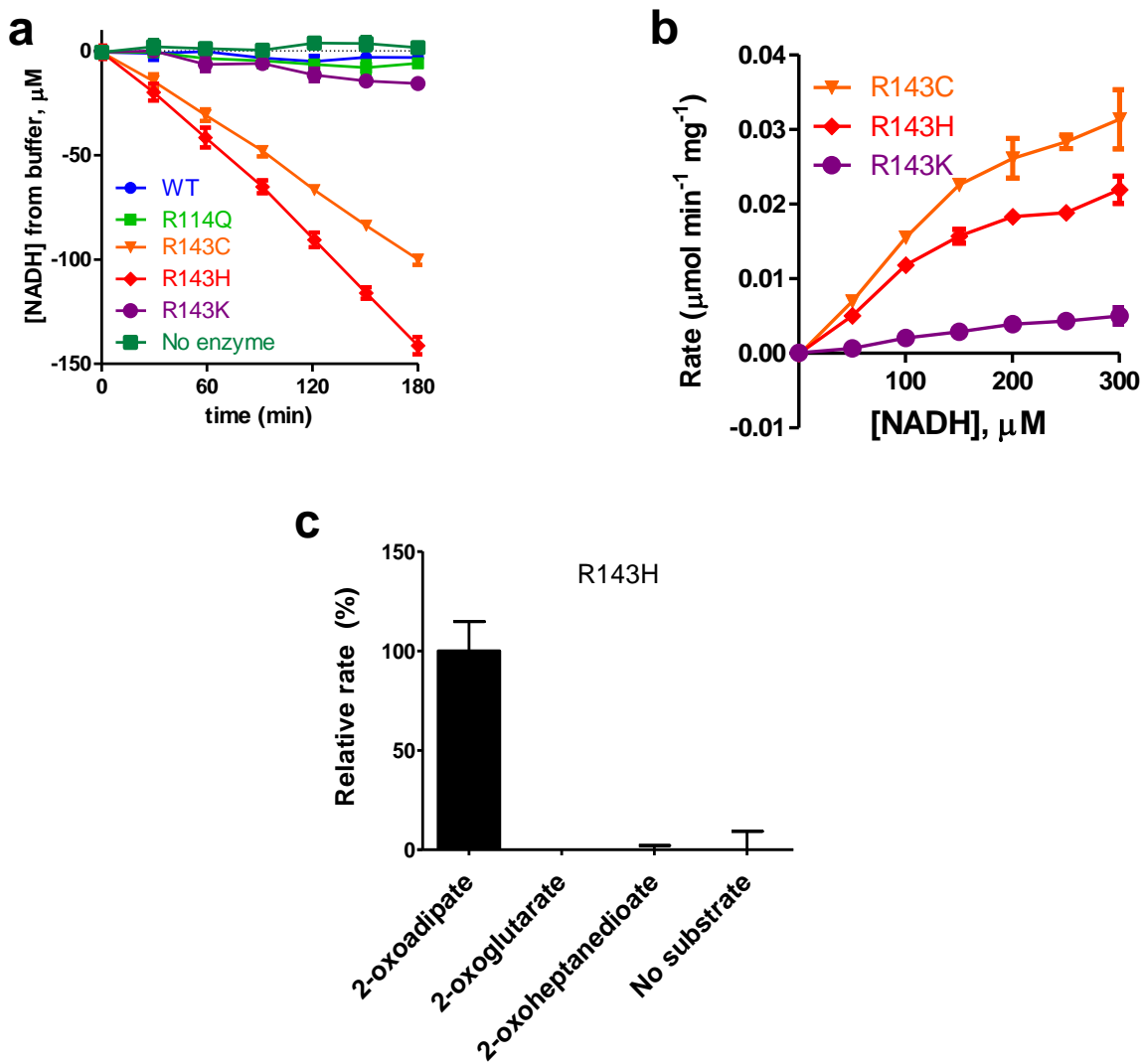
Supplementary Figure 1. Alignment of β -hydroxyacid oxidative decarboxylases.

Alignment of NADP⁺-dependent IDHs HsIDH1 and HsIDH2 that are mutated in human cancer with other β -hydroxyacid oxidative decarboxylases that act on (*R*)-hydroxyacid substrates, including an ancestral NADP⁺-dependent IDH from the proteobacteria *S. yanoikuya*e (Sy_IDH); NAD⁺-dependent IDHs from *H. sapiens*, *E. coli*, and *B. subtilis*; HIDHs from *S. cerevisiae*, *S. pombe*, *C. albicans*, and *T. thermophilus*; isopropylmalate dehydrogenases (IPMDHs) from *T. thermophilus*, *T. ferridoxans*, and *S. cerevisiae*; and tartrate dehydrogenases (TDHs) from *E. coli* and *P. putida*. Secondary structure elements from HsIDH1 are shown.



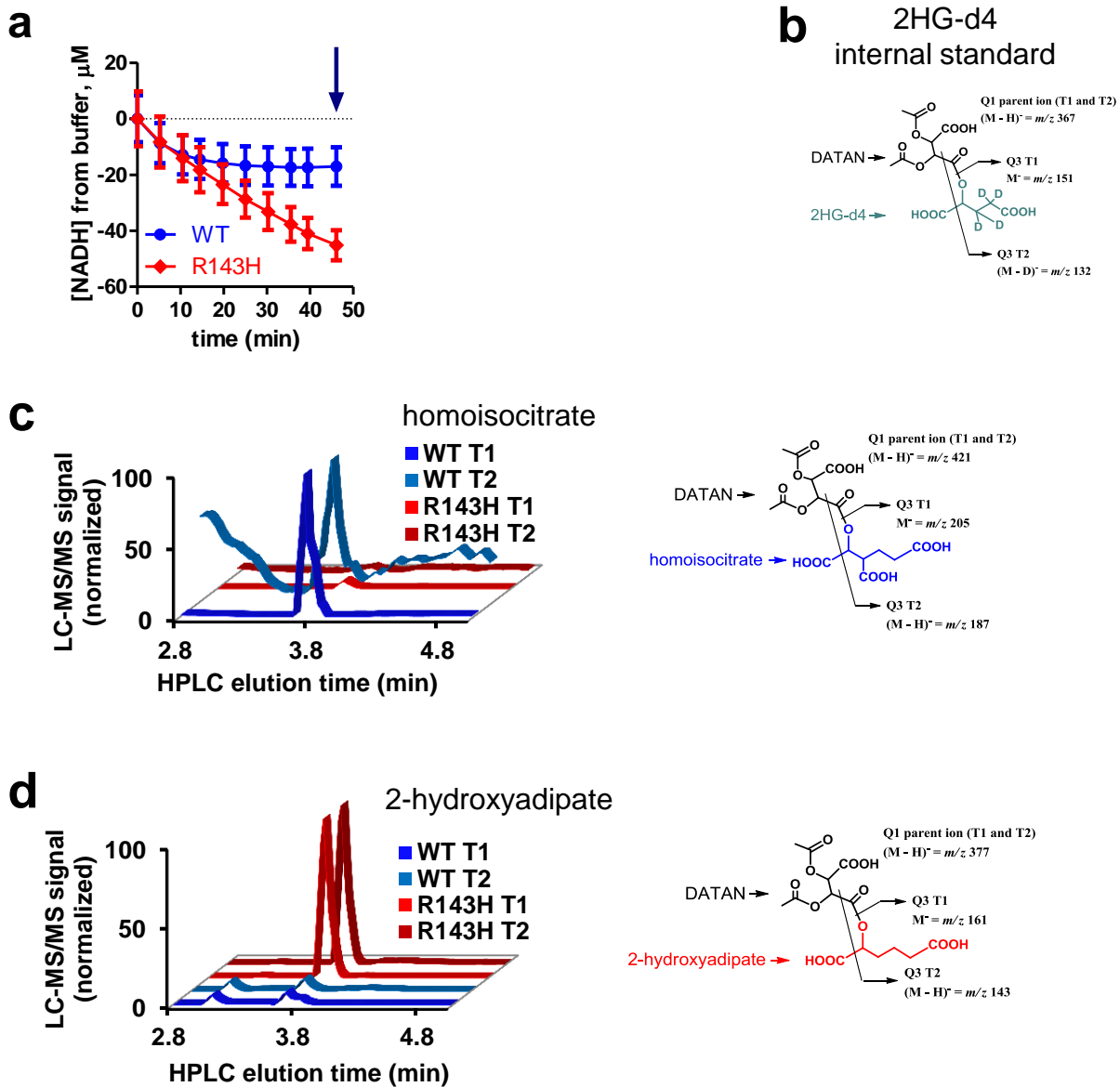
Supplementary Figure 2. Purification of *ScHIDH* mutants.

SDS-PAGE with silver stain of purified *ScHIDH* mutants. 15 µg of each purified protein were loaded.



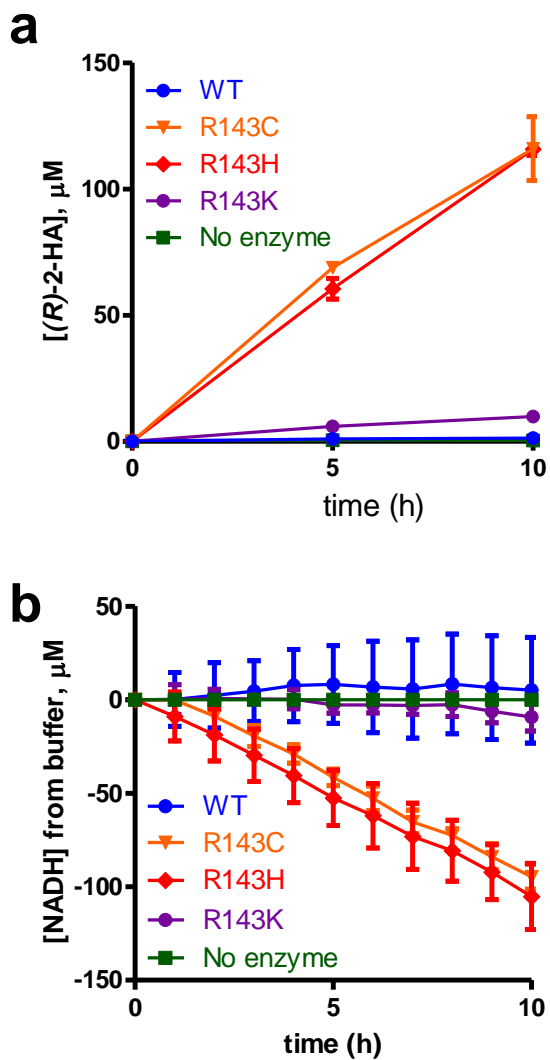
Supplementary Figure 3. Rate analysis of *ScHIDH* mutants.

(a) Decrease in NADH over time in reactions containing 10 mM 2-oxoadipate, 300 μM NADH, and the indicated *ScHIDH* mutant. (b) Initial rate of NADH decrease in reactions containing the indicated *ScHIDH* mutant and 0–300 μM NADH. (c) Initial rate of NADH decrease in reactions containing *ScHIDH*-R143H and 15 mM of either 2-oxoadipate, 2-oxoglutarate, or 2-oxoheptanedioate. Reactions contained 40 ng/ μl of the indicated purified enzyme, 15 mM 2-oxoadipate, 100 mM HEPES, pH 7.3, 20 mM MgCl₂, and 100 μM NADH unless otherwise specified. Rates are expressed either in $\mu\text{mol NADH min}^{-1} \text{mg}^{-1}$ enzyme, or in arbitrary relative rate of NADH decrease per unit time per unit of enzyme mass. Data are mean \pm s.d. ($n=2$) and are representative of three independent experiments.



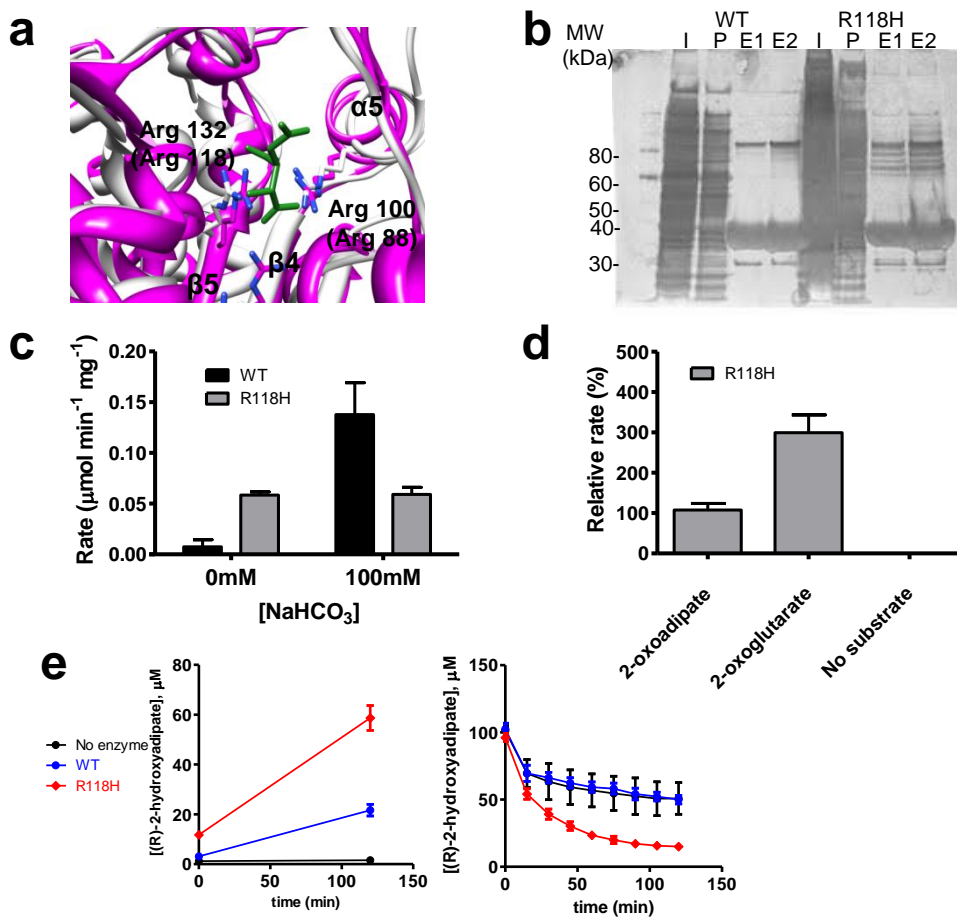
Supplementary Figure 4. LC-MS/MS analysis of *ScHIDH* reactions.

(a) NADH consumption was monitored in reactions containing 50 mM HEPES, pH 7.3, 5 mM MgCl₂, 50 mM NaHCO₃, 5 mM 2-oxoadipate, 100 μM NADH. After 45 min (arrow), [3,3,4,4]-²H₄-2-hydroxyglutarate (2HG-d4) internal standard was added and reactions were derivatized with diacetyl-L-tartaric anhydride (DATAN) and subjected to LC-MS/MS. (b) Fragmentation pattern for 2HG-d4, which was used as an internal standard to normalize the ion counts between different reactions. T1: Q1/Q3 (m/z) = 367.0/151.0, T2: Q1/Q3 (m/z) = 367.0/132.0. (c) Transitions (denoted T1 and T2) corresponding to homoisocitrate. T1: Q1/Q3 (m/z) = 421.3/205.1, T2: Q1/Q3 (m/z) = 421.3/187.0 as shown by the mass fragmentation diagram on the right. (d) Transitions corresponding to 2-hydroxyadipate. T1: Q1/Q3 (m/z) = 377.0/161.2, T2: Q1/Q3 (m/z) = 377.0/143.2 as shown in the mass fragmentation diagram on the right. Results are representative of two independent experiments. Data in (a) are mean \pm s.d. from two independent experiments.



Supplementary Figure 5. *ScHIDH* mutants stoichiometrically produce (R)-2-hydroxyadipate.

(a) (R)-2-hydroxyadipate concentration as quantified by LC-MS/MS for reactions initially containing 40 ng/ μl of the indicated *ScHIDH* mutant, 2 mM NADH, 2 mM 2-oxoadipate, 20 mM MgCl_2 , and 500 mM HEPES. **(b)** NADH concentration as assessed by absorbance at 340 nm for the same reactions. Data points are mean \pm s.d. from $n=3$ independent experiments.



Supplementary Figure 6. R118H mutation enhances *TtHIDH* (*R*)-2-hydroxyadipate dehydrogenase activity.

(a) Superimposition of three-dimensional structure of the active site for *TtHIDH*²⁵ (white) onto *HsIDH1*¹⁸ (pink; complex with isocitrate in green). *HsIDH1* residues Arg100 and Arg132 are shown and the corresponding residues for *TtHIDH* are shown in parentheses. **(b)** SDS-PAGE with silver stain of purified *TtHIDH* mutants. I, lysates induced to express protein; P, pass-through of lysate onto Ni-NTA column; E1, purified eluate 1; E2, purified eluate 2. **(c)** Addition of CO₂ to the reaction as 100 mM NaHCO₃ stimulates NADH consumption in the presence of *TtHIDH*-WT, but has no effect on NADH consumption in the presence of *TtHIDH*-R118H. **(d)** Relative rate of NADH consumption for reactions performed with either no substrate, 15 mM 2-oxoglutarate (5-carbons), or 15 mM 2-oxoadipate (6 carbons). **(e)** Concentration of (*R*)-2-hydroxyadipate and decrease in NADH from buffer for reactions containing *TtHIDH*-WT or *TtHIDH*-R118H. All reactions were performed at 45°C with 15 mM of 2-oxoadipate, 100 μM NADH, and 500 mM HEPES, pH 7.3, 20 mM MgCl₂ unless otherwise specified. Data are mean ± s.d. from n=2 reactions and representative of three independent experiments for (c) and (d), and from n=3 reactions and representative of two independent experiments for (e).

Supplementary References

24. Pettersen, E.F. et al. *J Comput Chem* **25**, 1605-1612 (2004).
25. Nango, E., Yamamoto, T., Kumasaka, T. & Eguchi, T. *J Biochem* **150**, 607-614 (2011).
26. Katoh, K. & Toh, H. *Briefings in bioinformatics* **9**, 286-298 (2008).
27. Gouet, P., Courcelle, E., Stuart, D.I. & Metoz, F. *Bioinformatics* **15**, 305-308 (1999).